BB

Michigan State University

National Superconducting Cyclotron Laboratory

CERN LIBRARIES, GENEVA
SCAN-9609075

SW9639

A LARGE BASIS SHELL MODEL ANALYSIS OF $^{14}N(\gamma,\pi^+)^{14}C_{gs}$ REACTION

S. KARATAGLIDIS, K. AMOS, C. BENNHOLD, and L. TIATOR

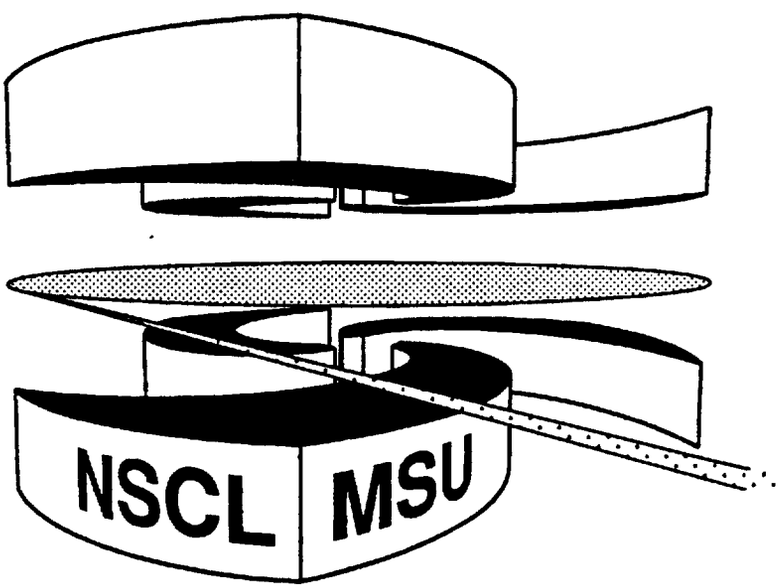

MSUCL-1020 **MARCH 1996**

MSUCL-1020

A large basis shell model analysis of $^{14}\mathrm{N}(\gamma,\pi^+)^{14}\mathrm{C}_{gs}$ reaction

S. Karataglidis

National Superconducting Cyclotron Laboratory, Michigan State University, East Lansing, MI, 48824-1321

K. Amos

School of Physics, University of Melbourne, Parkville, 3052, Victoria, Australia

C. Bennhold

Department of Physics, Center for Nuclear Studies, The George Washington University, Washington, D.C., 20052

L. Tiator

Institut für Kernphysik, Johannes Gutenberg-Universität, 55099 Mainz, Germany

(March 25, 1996)

Abstract

The $^{14}\mathrm{N}(\gamma,\pi^+)^{14}\mathrm{C}_{gs}$ cross section at $E_\gamma = 173$ MeV has been calculated using shell model wave functions determined in complete $(0+2)\hbar\omega$ and $(0+2+4)\hbar\omega$ shell model spaces. Using the $(0+2+4)\hbar\omega$ shell model wave functions yields an improvement over older results obtained with Cohen-Kurath wave functions by a factor of two, but still over-predicts the back-angle data. When correlated with analyses of inelastic electron and proton scattering from $^{14}\mathrm{N}$, the present results indicate the need for an improved shell model calculation and possibly

an improved description of the elementary pion production process in nuclei.

Typeset using REVTEX

Currently, microscopic model wave functions of the mass-14 nuclei belong to one of two classes. First, there are the conventional shell model wave functions that are obtained by adopting a model space for the structure and, within that space, diagonalising a suitable Hamiltonian. The $0\hbar\omega$ space wave functions of Cohen and Kurath (CK) [1] fall into this category, as do those of larger space models of Karataglidis *et al.* [2], Wolters *et al.* [3] ($(0+2)\hbar\omega$), and of Haxton and Johnson [4] ($(0+2+4)\hbar\omega$). The second class of model wave functions contains those constructed under the assumption that the wave functions may be specified completely by coupling two nucleon holes to a closed $0p$-shell and with amplitudes obtained by fitting to static properties of the mass 14 systems and from their use in analyses of elastic and inelastic electron scattering data. The wave functions of Ensslin *et al.* [5] and of Huffman *et al.* [6] (hereafter known as the $H1$ set) belong to this second class. However, there is a serious problem [7,8] with this (second) approach in that the Hamiltonian underlying the wave functions contains too large a value for the symmetry violating matrix element $\left\langle {}^3P_0 \middle| v \middle| {}^1S_0 \right\rangle$. The Hamiltonians for any of the $H1$ set of wave functions are in contradiction to the basic Mayer–Jensen shell model requirement of a strong spin–orbit interaction and some even place the single–nucleon $1p_{3/2}$ orbit with less binding than the $1p_{1/2}$ one [7]. Thus, this 'second' approach must be considered unphysical, and use of such wave functions in analyses of inelastic scattering data or of $(\gamma,\pi^{\pm})$ reactions is questionable. However, by design, these nuclear matrix elements do fit scattering data and may indicate what attributes of the more physical approach need to be addressed to improve the associated wave functions.

Extension of the shell model space beyond $0\hbar\omega$ produced significant improvement in the predictions of the $^{13}\mathrm{C}(\gamma,\pi^-)^{13}\mathrm{N}_{gs}$ [9]. The situation for the reaction $^{15}\mathrm{N}(\gamma,\pi^-)^{15}\mathrm{O}_{gs}$ is less understood due mostly to conflicting data sets [10]. Herein, we present the results of analyses of the cross sections from the photoproduction of charged pions from ^{14}N seeking to further constrain large space shell model specifications of the mass-14 wave functions in addition to those provided by evaluations of the Gamow-Teller (GT) matrix element for the β^--decay of ^{14}C, of the form factors from electron scattering and of the cross sections and

spin measurables from proton scattering data.

The GT matrix element for the β^--decay of ^{14}C and the ^{14}N$(\gamma,\pi^+)^{14}$C$_{gs}$ reaction both depend on the same (doubly reduced) one–body density matrix elements (OBDME). These are defined [11] by

$$\Psi_{JT}(j,j') = \frac{1}{\sqrt{(2J+1)(2T+1)}} \left\langle J_f\, T_f \left|\left|\left| \left[a^\dagger_{j'} \times \tilde{a}_j\right]^{JT} \right|\right|\right| J_i\, T_i \right\rangle . \tag{1}$$

They have been listed for the $0p$-shell in Table I in LS-coupled form, and as obtained from the CK $(8-16)$2BME wave functions, the $H1$ wave functions, the $(0+2)\hbar\omega$ wave functions obtained from the MK3W interaction [2], and the $(0+2+4)\hbar\omega$ wave functions obtained from the Haxton and Johnson (HJ) interaction [4]. The normalized GT matrix element [12] is defined by

$$R(GT) = \frac{\langle \Psi_f \,\|\sum_k \sigma(k) t_\pm(k)\|\, \Psi_i\rangle}{\sqrt{2J_i+1}\,|g_a/g_v|\,[3(2J_i+1)(N_i-Z_i)]^{1/2}} . \tag{2}$$

With $|g_a/g_v| = 1.264$, the values for each spectroscopy are given in the last row of Table I. Those values are to be compared with the value 0.0006 obtained from the measured β^--decay rate [12] which is anomalously low among p-shell nuclei. It has been suggested that meson exchange currents may play a role in this β^-–decay to account for the anomalously low rate [13].

An additional assessment of the various spectroscopies is provided by analysis of the inelastic $M1$ electron scattering form factor to the $0^+;1$ (2.313 MeV) state in ^{14}N (the isobaric analogue of the ^{14}C ground state). The form factor is displayed in Fig. 1, wherein the data of Huffman *et al.* [6] (squares) and Ensslin *et al.* (crosses [5] and circles [14]) are compared to the results of calculations made using the $(0+2+4)\hbar\omega$ wave functions (solid line), CK wave functions (long–dashed line), $(0+2)\hbar\omega$ wave functions (dot-dashed line), and $H1$ wave functions (short–dashed line). All calculations were made assuming a nuclear current of one–body form [15]. The calculation made using the $H1$ wave functions does best of all in comparison to the data, but those wave functions were specifically designed to fit these data. Of the calculations made using the shell-model spectroscopies, that using the

$(0+2+4)\hbar\omega$ wave functions shows best agreement with data, reducing the discrepancy from a factor of 4, as in the case of the CK calculation, to a factor of 2. In order to reproduce the data, both Amos *et al.* [8] and Doyle and Mukhopadhyay [16] reduced the $L = 2$ OBDME by a factor of 2. The result obtained using the $(0 + 2)\hbar\omega$ wave functions has a different variation with (low) momentum transfer values from the other results.

Clearly, the inclusion of higher $\hbar\omega$ components in the shell model wave functions is equivalent to some aspects of the core polarization corrections one adopts to bring the smaller basis CK structure results into agreement with observation. Yet the match to the data is still far from satisfactory. However, transverse magnetic form factors from electron scattering are expected to be strongly influenced by meson exchange currents (MEC). MEC contributions involve two–body density matrix elements and each type of meson exchange amplitude must be evaluated independently. One cannot use the continuity equation and Siegert operators as is the case for electric transverse form factor analyses [17]. To the extent that MEC effects are important, the fit found with the $H1$ set of functions to this $M1$ form factor would have to be considered inappropriate. Furthermore, the form factor should not be used naively to specify core polarization renormalization upon smaller basis shell model structures. However, MEC effects of such nature are not of importance in analyses of inelastic proton scattering and calculations made of the excitation of the $0^+;1$ state at 2.313 MeV by 122 and 160 MeV protons [8] indicated that the core polarization corrections required to fit those data were predominantly associated with the $L = 2$ transition amplitudes but were not the same as needed with the (CK) spectroscopy to fit the electron scattering form factor. Only recently [2] has it been possible to analyze proton scattering data with a fully microscopic distorted wave approximation including a realistic medium modified effective NN interaction and with larger space structure models. In particular, that approach was used to analyze the cross section and analyzing power from 160 MeV inelastic proton scattering to the $0^+;1$ (2.313 MeV) state in ^{14}N. That study found quite poor results when the $(0 + 2)\hbar\omega$ model OBDME were used, but quite reasonable ones when the $(0 + 2 + 4)\hbar\omega$ spectroscopic information is input to the calculations. The large basis structure results fit the large angle

(high momentum transfer) (p,p') cross sections quite well and were the only ones able to reproduce the structure of the analyzing power data. The (p,p') cross section indicates in particular that the $L=2$ OBDME from the $(0+2+4)\hbar\omega$ wave functions are reasonable.

Thus, as the electron scattering form factor (dominated by the $L=2$ attributes in the OBDME structure) and the inelastic proton scattering results do not concur, and as the GT matrix elements largely reflect the $L=0$ OBDME in the structure, we have turned to an analysis of the $^{14}\mathrm{N}(\gamma,\pi^+)^{14}\mathrm{C}_{gs}$ cross section seeking an independent assessment of the quality of the shell model structure wave functions. In analyses of nuclear photoproduction of pions, the elementary pion production operator of Blomqvist and Laget (BL) [18] is commonly adopted. This operator contains the Born terms for the elementary process as well as the Δ-resonance contribution, and part of its value for use in nuclear calculations is that it is cast in a frame–independent fashion. For most low-energy calculations of nuclear charged pion photoproduction [11] the Kroll-Ruderman (KR) term [19]; a term proportional to $\boldsymbol{\sigma}\cdot\boldsymbol{\varepsilon}$ and related to the GT matrix element, usually dominates. However, in the case of $^{14}\mathrm{N}(\gamma,\pi^+)^{14}\mathrm{C}_{gs}$, due to the small GT matrix element for the β^--decay of the ^{14}C ground state, the KR term is suppressed. In that circumstance, the reaction can become sensitive to details of the description of the elementary production process, such as different nonrelativistic reductions, unitarity constraints, cross channel Δ exchange. Some of these issues were studied by Wittman and Mukhopadhyay [20] and found to be on the order of at most 30% at low energies. Improved versions of the elementary pion photoproduction process exist [21] but they are usually cast in the barycentric frame and so additional frame transformations are needed to properly treat the motion of the nucleons within the nucleus. Consequently, we continue using the BL operator here in the interests of simplicity and to assess the effects of improved shell model structures against results reported previously, and based upon the formalism of Tiator and Wright [11]. Such previous calculations of the low-energy $^{14}\mathrm{N}(\gamma,\pi^+)^{14}\mathrm{C}_{gs}$ cross section made using the CK wave functions [22,23] severely overestimate the cross section (by up to a factor of 4).

The results of our calculations of the $^{14}\mathrm{N}(\gamma,\pi^+)^{14}\mathrm{C}_{gs}$ cross section for an incident photon

energy of 173 MeV are compared with the data of Röhrich *et al.* [22] in Fig. 2. The results of the calculations made using the $(0+2+4)\hbar\omega$, the CK $(8-16)$2BME, the $(0+2)\hbar\omega$ and the $H1$ wave functions are displayed therein by the solid, dashed, dot–dashed and dotted lines respectively. Harmonic oscillator functions with the oscillator length set to 1.64 fm [2] were used to represent the single particle bound states. The results obtained by using the $H1$ set of wave functions gives best agreement with the data. The calculation based on the CK $0p$-shell model does worst of all, overestimating the small-angle cross section by a factor of 2 and the larger angle cross section by a factor of 4. The wave functions of García and Brown [24], which were obtained from $0p$-shell model wave functions with $2\hbar\omega$ admixtures added perturbatively, and which fitted the inelastic M1 electron scattering form factor, gives a result similar to the CK one, and so is not displayed. The calculation using the $(0+2)\hbar\omega$ wave functions is smaller than the CK result by about 20% at large scattering angles, but at the expense of losing the shape of the cross section in the region of the minimum near 50°. A similar (erroneous) enhancement in this region of momentum transfer was noticed in the inelastic proton scattering cross section to the $0^+;1$ (2.313 MeV) state in ^{14}N calculated using those OBDME [2]. The reduction brought about by the use of the $(0+2+4)\hbar\omega$ wave functions is the most significant among the various shell model calculations essentially being a factor of 2 smaller than CK result. The $(0+2+4)\hbar\omega$ space prediction is in near agreement with the data at small scattering angles.

The cause of the reduction of the cross section at large angles produced by using the $(0+2+4)\hbar\omega$ wave functions (in comparison to use of the CK ones) is illustrated in Fig. 3, wherein the total cross section and contributions from the $L=0$ and $L=2$ components are displayed by the solid, long dashed and dot-dashed lines, respectively. The $L=2$ component obtained from the CK wave functions is displayed by the small dashed line. There is little difference between the $L=0$ component of the $0p$-shell model calculation and the $(0+2+4)\hbar\omega$ shell model calculation, and so the CK result for that component is not displayed. This equivalence is consistent with the results of the calculations of the GT matrix element as that matrix element is related to the $L=0$ part of the cross section.

The cross section at small angles is due to constructive interference between the $L = 0$ and $L = 2$ terms. This interference becomes destructive at around 50° and is responsible for the observed minimum. At large angles, the $L = 2$ contribution to the cross section so dominates that it is the sole important attribute, and so sets the difference between the individual shell model predictions.

In conclusion, the $E_\gamma = 173$ MeV $^{14}\mathrm{N}(\gamma,\pi^+)^{14}\mathrm{C}_{gs}$ cross section has for the first time been predicted using $(0+2+4)\hbar\omega$ wave functions, as obtained with the Haxton and Johnson interaction. A general reduction in the cross section has been observed over all angles in comparison to the results obtained using the 0*p*-shell model spectroscopy. This suffices to bring the calculation to within a factor of 2 of the data; a mismatch consistent with the (one–body operator) predictions of the transverse magnetic form factor from electron scattering. The reduction is a result of an overall reduction in the $L = 2$ component of the cross section. The remaining discrepancy may reflect problems with the HJ interaction, but, given the analyses of inelastic proton scattering to the $0^+;1$ (2.313 MeV) state in ^{14}N, such problems should not be severe. One will need to use improved models of the reaction processes for the electromagnetic interaction processes, accounting for MEC at the very least with the electron scattering form factors and perhaps improving the description of the elementary pion photoproduction process.

ACKNOWLEDGMENTS

The authors wish to thank W. C. Haxton for helpful discussions. Support is acknowledged for LT by the Deutsche Forschungsgemeinschaft (SFB201), and for CB by DOE grant DE-FG02-95-ER40907. This work was also supported by NSF Grant No. PHY94-03666 (MSU).

REFERENCES

[1] S. Cohen and D. Kurath, Nucl. Phys. **73**, 1 (1965).

[2] S. Karataglidis, P. J. Dortmans, K. Amos, and R. de Swiniarski, Phys. Rev. C **53**, 838 (1996).

[3] A. A. Wolters, A. G. M. van Hees, and P. W. M. Glaudemans, Phys. Rev. C **42**, 2053 (1990); *ibid*, Phys. Rev. C **42**, 2062 (1990).

[4] W. C. Haxton and C. Johnson, Phys. Rev. Lett. **65**, 1325 (1990).

[5] N. Ensslin, W. Bertozzi, S. Kowalski, C. P. Sargent, W. Turchinetz, C. F. Williamson, S. Fivorzinsky, J. Lightbody, and S. Penner, Phys. Rev. C **9**, 1705 (1974).

[6] R. L. Huffman, J. Dubach, R. S. Hicks, and M. A. Plum, Phys. Rev. C **35**, 1 (1987).

[7] I. Talmi, Phys. Rev. C **39**, 284 (1989).

[8] K. Amos, D. Koetsier, and D. Kurath, Phys. Rev. C **40**, 374 (1989).

[9] C. Bennhold and L. Tiator, Nucl. Phys. **A519**, 805 (1990).

[10] C. Bennhold, L. Tiator, S. Kamalov, and R. Mach, Phys. Rev. C **46**, 2456 (1992).

[11] L. Tiator and L. E. Wright, Phys. Rev. C **30**, 989 (1984).

[12] W.–T. Chou, E. K. Warburton, and B. A. Brown, Phys. Rev. C **47**, 163 (1993).

[13] B. Goulard, B. Lorazo, H. Primakoff, and J. D. Vergados, Phys. Rev. C **16**, 1999 (1977).

[14] N. Ensslin, L. W. Fagg, R. A. Lindgren, W. L. Bendel, and E. C. Jones, Jr., Phys. Rev. C **19**, 569 (1979).

[15] T. deForest, Jr. and J. D. Walecka, Adv. Phys. **15**, 1 (1966).

[16] B. C. Doyle and N. C. Mukhopadhyay, Phys. Rev. C **52**, 1947 (1995).

[17] S. Karataglidis, P. Halse, and K. Amos, Phys. Rev. C **51**, 2494 (1995).

[18] K. I. Blomqvist and J. M. Laget, Nucl. Phys. **A280**, 405 (1977).

[19] N. M. Kroll and M. A. Ruderman, Phys. Rev. **93**, 233 (1954).

[20] R. Wittman and N. C. Mukhopadhyay, Phys. Rev. Lett. **57**, 1113 (1986).

[21] Y. Surya and F. Gross, CEBAF preprint, submitted to Phys. Rev. C.

[22] K. Röhrich, L. Tiator, G. Köbschall, Ch. Reifferscheid, Ch. Schmitt, V. H. Walther, K. Weinand, and L. E. Wright, Phys. Lett. **153B**, 203 (1985); K. Röhrich, G. Köbschall, C. Reifferscheid, C. Schmitt, V. H. Walther, and K. Weinand, Nucl. Phys. **A475**, 761 (1987).

[23] D. Koetsier, K. Amos, L. Tiator, C. Bennhold, and L. E. Wright, Phys. Rev. C **45**, 230 (1992).

[24] A. García and B. A. Brown, Phys. Rev. C **52**, 3416 (1995).

FIGURES

FIG. 1. Transverse $M1$ electron scattering form factor to the $0^+;1$ (2.313 MeV) state in ^{14}N. The data of Huffman *et al.* [6] (squares) and of Ensslin *et al.* [14] (circles) and [5] (crosses) are compared to the results of one–body calculations made using the $(0+2+4)\hbar\omega$ wave functions (solid line), CK wave functions (long-dashed line), $(0+2)\hbar\omega$ wave functions (dot-dashed line), and $H1$ wave functions (short-dashed line).

FIG. 2. The $^{14}\mathrm{N}(\gamma,\pi^+)^{14}\mathrm{C}_{gs}$ differential cross section at $E_\gamma = 173$ MeV. The data of Röhrich *et al.* [22] are compared to the results of the calculations using the $(0+2+4)\hbar\omega$ wave functions (solid line), the CK wave functions (long dashed line), the $(0+2)\hbar\omega$ wave functions (dot-dashed line) and the $H1$ set of wave functions of Huffman *et al.* [6] (short dashed line). Harmonic oscillator single particle wave functions were used in the calculations.

FIG. 3. The $L = 0$ (long dashed line) and $L = 2$ (dot-dashed line) contributions to the $^{14}\mathrm{N}(\gamma,\pi^+)^{14}\mathrm{C}_{gs}$ cross section (solid line) at $E_\gamma = 173$ MeV, calculated using the $(0+2+4)\hbar\omega$ wave functions. The $L = 2$ component of the CK result is also shown (short dashed line). The data are those of Röhrich *et al.* [22].

TABLES

TABLE I. The doubly-reduced OBDME, $\Psi_{JT}(\alpha',\alpha)$, for the transition $^{14}\mathrm{N}_{gs} \rightarrow {}^{14}\mathrm{C}_{gs}$, given in LS-coupled form. The results from the $(0+2)\hbar\omega$ calculation (MK3W) are compared with those from the $(0+2+4)\hbar\omega$ calculation (Haxton), from the CK calculation and from the Huffman $H1$ calculation [6]. Only those transitions in the $0p$-shell are listed but the complete sets were used to evaluate the normalized GT matrix elements, $R(GT)$ given in the last row.

L,S	MK3W	Haxton	CK	H1
0,1	−0.06643	−0.02954	−0.02937	−0.033
1,0	−0.22075	0.22131	0.31973	0.339
1,1	0.11699	−0.07107	−0.10188	0.046
2,1	−0.74047	0.61758	0.83687	0.434
R(GT)	0.1151	0.0846	−0.0505	−0.058[a]

[a]Ref. [6]

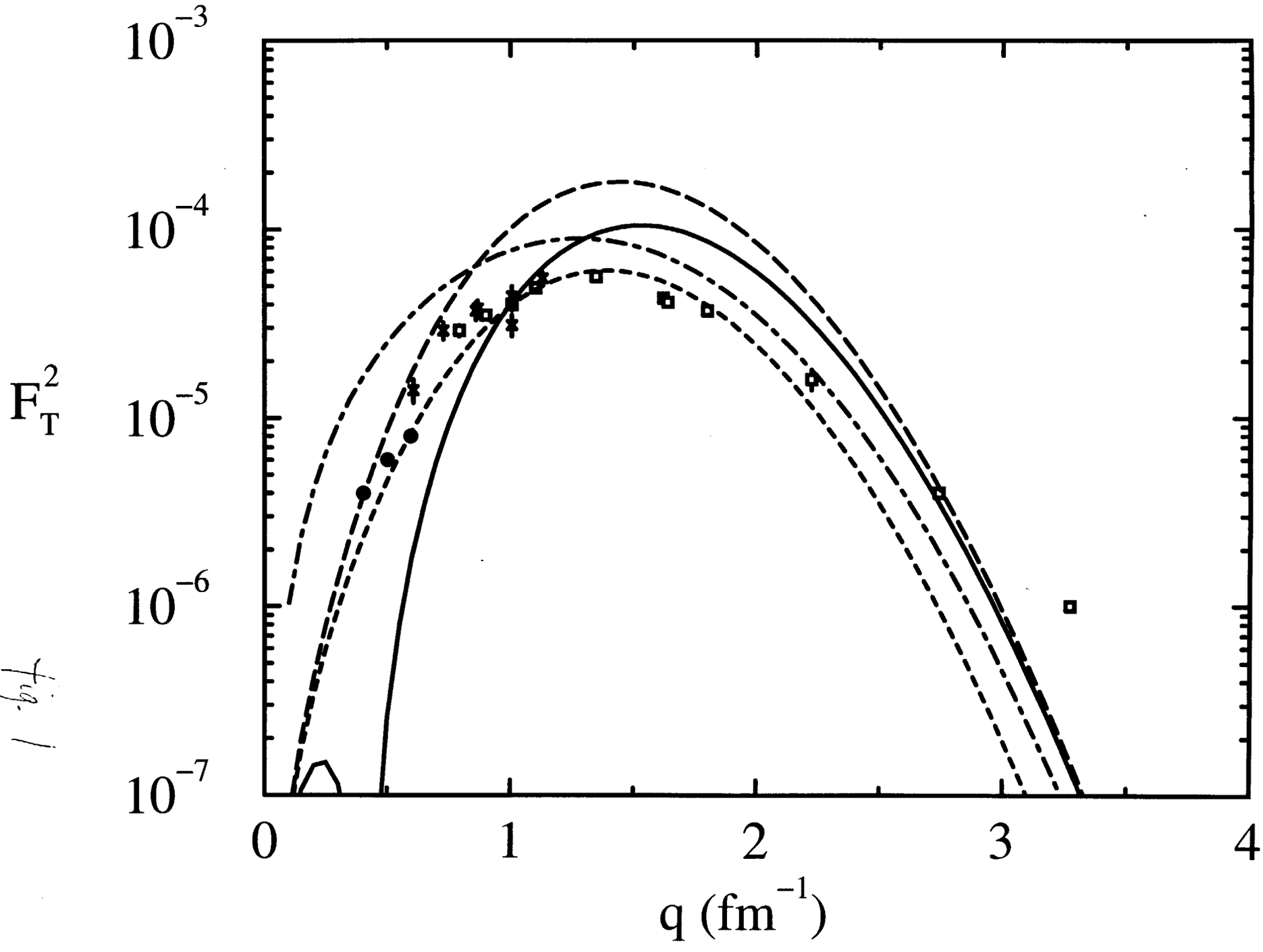

fig. 1

fig. 2

fig. 3

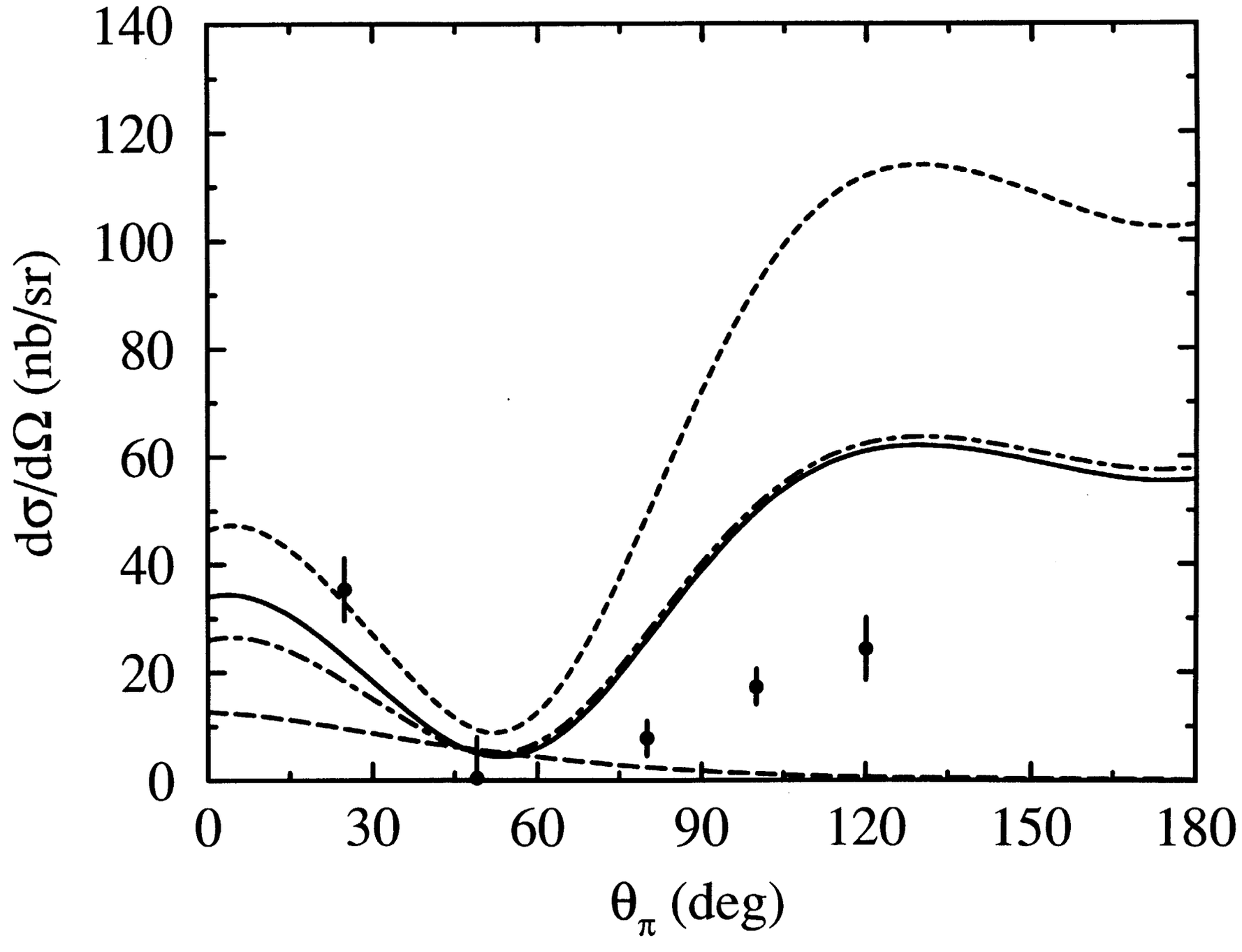

fig. 3